Thick Film Sensors for Soil Measurements

Gerardo Espindola Garcia, John Atkinson and Joel Smethurst
Faculty of Engineering and Environment
University of Southampton
Southampton, United Kingdom
Email: Gerardo.Espindola@soton.ac.uk, jka@soton.ac.uk, j.a.smethurst@soton.ac.uk

***Abstract*—Water content has considerable influence on soil pore water pressure and shear strength, potentially leading to failure in earthworks. This research aims to develop novel sensors (employing Thick-Film electrodes) intended to detect changes in soil parameters such as resistivity, porosity and water content and determine if these are indicative of earthworks instability (potential slope failure). Using Thick Film electrodes to measure parameters could be a cost effective method for condition monitoring. The resistivity output of the sensors and how it relates to the soil water content needs to be understood, and a framework of working conditions for this sensing technology needs to be documented. In this study, the behaviour of the Thick Film cell developed by the University of Southampton was tested for a particular soil particle size by simulating heavy rainfall and rising of the water table within a soil column. Final results show a consistent response from Thick Film cell for the specific soil sample used, however, the direction of infiltration has created a very interesting difference in resistivity readings that need to be further investigated.**

Keywords- thick film; soil resistivity; water content.

I. INTRODUCTION

Landslides due to heavy rainfall have been a concern in the UK in recent times, particularly in 2012, when several incidents caused trains to derail, including Beaminster tunnel in Dorset, St Bees station in West Cumbria, and the West Highland line near Tulloch, among others. Not only is the safety of people a concern but also the cost of disruption to the rail transport system. As in most developed countries, the earthworks in the UK supporting the transport system are at risk due to ageing and a lack of maintenance and renovation due to the high costs involved [1].

However, predicting landslips has several difficulties. A significant part of the railway infrastructure dates from the Victorian age (the mid-nineteenth century), and this infrastructure does not comply with present design standards. In the period 1834 to 1841, around 1060km of railways were built in the UK following nine main lines. Pick and shovel excavations were used to build most of the soil cuttings and embankments, with the latter often poorly compacted, and heterogeneous in composition [2]. Vegetation and climate can modify the soil water content causing shrink and swell cycles, which will affect the strength of the soil. Natural weathering processes also occur and vary with rainfall, extreme temperatures and biological activity. Additionally, increases in the speed and weight of railway traffic affect applied loads and earthworks performance [3].

Railway earthwork failures can have impacts on railway operations, involving partial or total disruption of the rail network. Remediation implies significant cost, including the direct cost of reconstruction, and fines incurred by the track operator for unexpected line closure or delays to trains. Therefore, to prevent as much as possible reaching a state where they may fail and need to be remediated, a more effective and accurate condition monitoring of assets needs to be designed and developed, targeting smaller, low-cost and simpler sensing devices. Condition monitoring should enable more targeted interventions for earthworks. There is evidence that proactive maintenance can reduce the total cost of unplanned repairs considerably, reducing cost by about 60% per metre for London Underground Limited (LUL) [2].

This work tries to relate the water content of the soil with the soil resistivity/conductivity using printed Thick Film (TF) sensors, to develop a sensor device to infer changes in the soil structure due to water cycles using these parameters. Thick film sensing has been used for other applications such as water quality and other soil measurements [4]-[6].

The soil water content (θ) is defined as the amount of water that is removed when a soil sample is heated at over 100ºC until the maximum weight loss is reached. This parameter is commonly measured in the environmental field such as ecology and hydrology including agriculture [7]-[10], and along with electrical conductivity in many geotechnical applications [11]-[13].

The Electrical Conductivity (EC) of the soil is defined as the reciprocal of the soil's resistivity, which is linked to the electrical resistance that can be deduced between two electrodes in a conductive material on application of a known voltage. There are three possible ways that the current is able to flow in soils, and these are shown in Figure 1. The first path is a solid-liquid segment where an exchange of cations is associated with clay minerals.

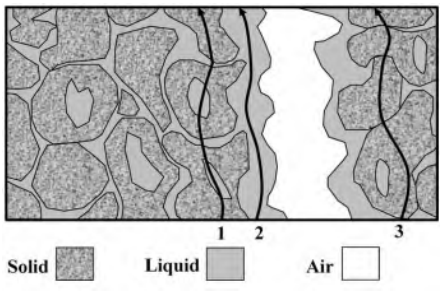

Figure 1. Soil sample cross section with pathways of EC [14].

The second is related to current flow in the liquids due to the presence of dissolved particles in the water, and the last is the flow in solids in direct contact with each other [14]. A key consideration for the TF sensor electrode arrangement is the potential heterogeneity of the soil, in terms of particle sizes and the way they pack around the sensor. A large spacing between electrodes is desirable to monitor larger and more representative volume of soil, but this can generate measurement noise due to the increase of the length of the electrical path between electrodes [15]. Soil resistivity/conductivity has been directly studied and linked to water content and used for measurement and assessment of seasonal water cycles on soil slope stability. A recent study using a clay soil performed by Hen-Jones et al. (2017) [3] showed an inverse relationship between soil resistivity and water content in both laboratory and field experiments which cycled water content (Figure 2) [3][16]. The instrumentation used included the Decagon 5TE sensor which uses a stainless steel electrode array to measure soil EC, temperature and water content directly. As the Decagon 5TE sensor requires good contact between the electrodes and the soil, the electrodes were coated with a layer of Nyogel 756 during the experiments.

The electrical resistivity in soil samples has also been investigated by McCarter (1984) [16] for compacted clay, including responses of different degrees of compaction and saturation. Figure 3a clearly shows that resistivity decreases quickly at high water contents and the rate of change almost flattens when water content exceeds 20%. Its reciprocal, the soil conductivity is shown in Figure 3b, in electrostatic units σ_{esu} ($\sigma_{esu}=1/\rho \cdot 9x10^9$).

The electrical conductivity of the soil (σ) is defined as the reciprocal of the soil's resistivity (ρ) which is linked to the electrical resistance (R) given by the equation:

$$\text{Resistance (R)} = V/I \quad (1)$$

The voltage (V) can be measured across a pair of electrodes by manipulation of the current, namely a drive current (I); this resistance generally is a function of the geometry of the electrodes (Cell), which includes the cross-sectional area (A) (of the electrical conductivity electrodes) and length (L) between the electrodes (of the material being measured).

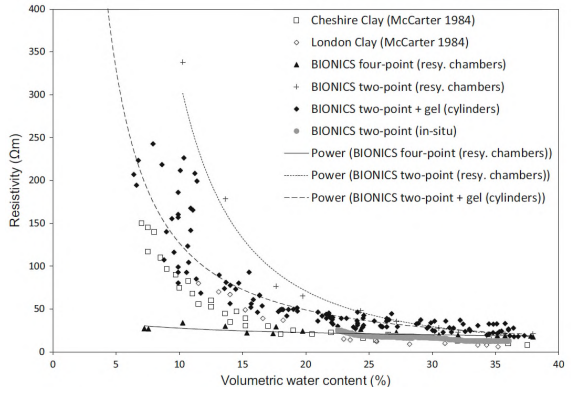

Figure 2. Water content - resistivity relationships [3]

With these known parameters a cell constant can be calculated by the following relationship:

$$\text{Cell Constant (K)} = A/L \quad (2)$$

Thus, the resistivity is expressed as follows:

$$\rho = R \cdot K \quad (3)$$

Conductivity is expressed as follows:

$$\sigma = 1/(R \cdot K) \quad (4)$$

The apparatus, characteristics of the soil sample, TF cell parameters and the methodology used are described in Section 2. Table 1 lists the three different sets of experiments that were conducted. The results of each set of experiments are discussed in Section 3, including preliminary Tests used to obtain the initial set up. Finally, Section 4 gives some remarks and future work to follow given the results obtained.

II. METHODS

The general aim of the set of experiments included in this paper is to characterise the response of the Thick Film cell when used to determine the resistivity of a soil sample subjected to a simulation of seasonal wetting processes. The TF cell output voltage is used to calculate resistivity and conductivity of the soil sample over consecutive cycles of wetting and drying.

TABLE I. EXPERIMENT DATASETS DESCRIPTION

Name	Experiment Description		
	Drive Current	***Filling Direction***	***Draining Direction***
Preliminary 1 - 500	500 µA	Top → Bottom	Top → Bottom
Preliminary 2 - 250	250 µA	Top → Bottom	Top → Bottom
Test 1- Orientation	250 µA	Top → Bottom	Top → Bottom
Test 2- Location a	250 µA	Top → Bottom	Top → Bottom
Test 2- Location b	150 µA	Top → Bottom	Top → Bottom
Test 3- Wetting	150 µA	Bottom →Top	Top → Bottom

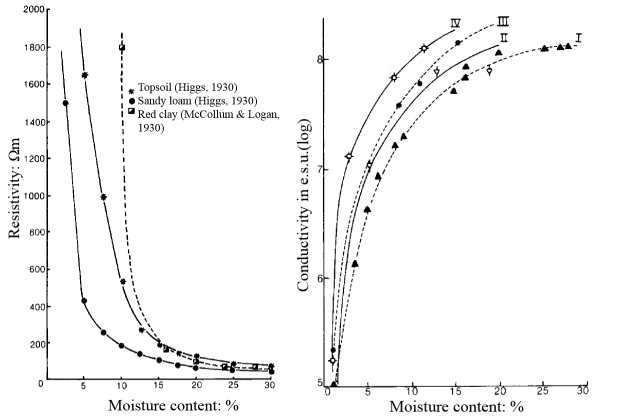

Figure 3. Variation in soil resistivity (a) and soil conductivity (b) with water content [16].

A. Apparatus

In order to achieve this goal, a series of laboratory experiments were conducted, using a column of 1.0m height and 0.255m diameter, with a geotextile and gravel filter layer at the base to avoid clogging of the drainage pipe. Following in part the methodology described by Sophocleous & Atkinson (2015) [15], the soil column was used to bury the Thick Film (TF) cell at the same depth as a soil water content probe (a Delta-T Devices ML2x Theta probe), at 0.20m above the geotextile filter in the bottom of the column. A schematic representation of this apparatus is shown in Figure 4. The GP1 Data Logger by Delta-T Devices™ was used as an instrumentation interface.

For all the laboratory experiments, the soil samples were subjected to complete cycles of water variation consisting of wetting (imbibition) phase followed by a draining phase. Measurements of water content and TF cell output voltage were recorded simultaneously, and full cycles are plotted and analysed.

One full cycle started when water was poured directly into the top of the column, and wetting continued until the Theta probe reached maximum water content and a column of water of 0.15m height had formed above the soil sample. The draining phase was continued for 24 hours after the bulk of the water in the column had drained out. Some water continued to drain until the water content reached about 10% after the first 4 ~ 6 hours. An average of 36% was recorded as maximum water content, with minimum values of the water content of 10-12%, as the soil retained some pore water that was not able to drain under gravity.

B. Sample particle size

The pluviation tube method was used to fill the column using fraction D of Leighton Buzzard quartz sand. This sand has particle sizes ranging from 150μm to 300μm. However, it was observed that after several consecutive cycles of wetting and drying the sand reorganised its particle size distribution, moving smaller particles to the bottom of the column. Therefore a particle size distribution test was made at the end of each set of experiments to determine sizes around the location of the sensors. The column was re-built after each test listed in Table 1.

C. Thick Film cell and drive current

The TF cell (Figure 5) used for the experiments compensates some of the drawbacks of an earlier conductivity sensor design used for soil monitoring by using the principle of ratio-metric symmetry (a balance between spacing and cross-sectional area) in the configuration of the electrodes [15]. The TF cell configuration is shown in Figure 5a. The screen printed electrodes are of gold isolated by a waterproofing layer, with two sets of electrodes placed parallel to one another using a custom 3D printed structure (Figure 5b). The structure allows space for the sample material to be inserted between the sets of electrodes.

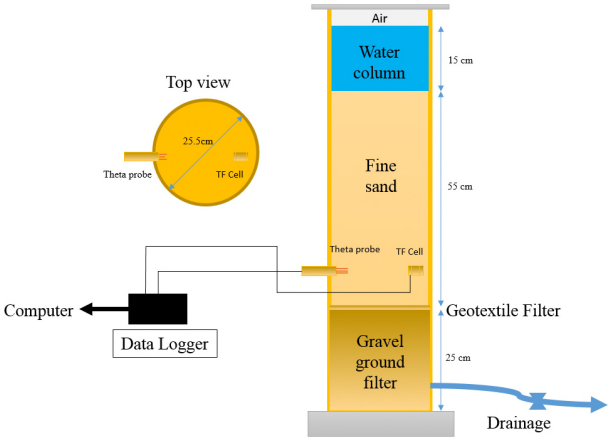

Figure 4. Schematic of apparatus used for experiments.

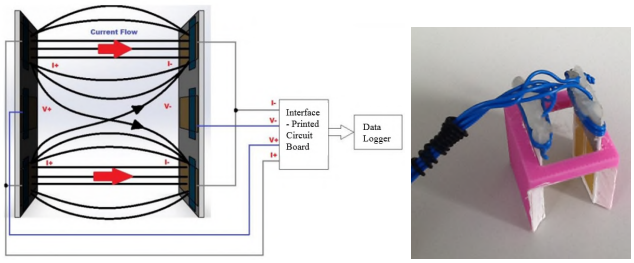

Figure 5. (a) TF Cell configuration [15] (b) TF cell 3D printed structure for the TF electrodes.

Each set is composed of 3 electrodes, where the outer electrodes are driving the current, and the potential of the cell is measured through the inner electrode on each set. The TF cell is interfaced by a low power electrical circuit designed to generate a voltage for conductivity, and the data logger easily reads this conductivity as a function of output voltage. This interface circuit allows the AC drive current amplitude to be varied up to 10mA.

D. Experiments carried out

For Test 1 and Test 2a, the drive current used to configure the Thick film cell was 250μA, while for Test 2b and 3 it was changed to 150μA, as this was found to be the lowest value giving a stable reading of the TF cell.

For Test 1, 2a and 2b the column was filled at the top of the apparatus allowing the water to drain at the bottom. Only in Test 3, the water was pumped upwards from the bottom, followed by draining at the base as in the rest of the tests (see Table 1).

For Test 1, the orientation of the Theta probe was changed to vertical. For the rest of the experiments, the Theta probe was restored to the original horizontal position. Both sensors, Theta probe and TF cell were physically closer together for Tests 2a, 2b and 3 than for the preliminary tests and Test1, which helped to give more consistent readings.

 ISBN: 978-1-61208-581-4

III. RESULTS

All water content values presented refer to volumetric water content, which corresponds to the parameter that is commonly used in literature and is therefore applicable for comparison purposes. Preliminary experiments used induced currents (drive current) of 500µA and 250µA respectively, and sensor responses were compared. These initial tests had the objective of providing the basic set-up of the TF cell.

The first set-up configuration using a drive current of 500µA proved to be inappropriate to obtain the full response during the wetting phases (labelled 1 on the graphs). As the soil sample reached maximum water content (~34%), the TF output voltage suddenly dropped, in addition, very inconsistent responses were recorded during the draining phases (labelled 2 on the graphs); the voltage data were converted to resistivity, and this is plotted in Figure 6. The range of operation for this configuration was recorded as resistivity from ~260Ωm to 360Ωm.

For the second set-up using a drive current of 250µA, the response for the wetting phases was improved, giving a complete set of measurements during wetting. Figure 7 shows the TF cell resistivity response, where it is evident that the response over consecutive cycles continued to be dispersed for both phases but more prominently in the wetting phases.

The improvement compared to the previous set-up is notable, but there is still a sharp change when the soil sample reaches a water content over 33%. Nonetheless, it is less variable than that of the response using 500µA. Therefore 250µA was chosen as the starting level of drive current to continue investigating the TF cell response, this time modifying other parameters.

For all cycles, the voltage (V) applied to the cell and the cell constant (K) were kept the same; 5V was the maximum valid output voltage for the interface circuit of the Thick film conductivity sensor, which also had a cell constant value of 1/15m. Readings from the Theta probe and TF cell were taken at intervals of 5 seconds. The first cycles of all tests were removed as the readings are considered outliers due to the initial dry condition of the sand (which gave a measured value of less than 0.1% water content).

Only three cycles are presented on each of the following plots for better visualisation, and in most cases, the re-wetting and re-draining cycles plotted are those that immediately followed cycle 1.

A. Test 1

Figure 8 shows the resistivity- water content curves of three of the five cycles made for Test 1. It can be observed that there is better repeatability over the draining phases than the wetting phases compared with the 250µA preliminary test. The sudden change in resistivity at higher water content (greater than 33%) was also no longer observed. Resistivity remains almost flat above 22% water content on all drying cycles and grows exponentially when the water content is below that value. Responses during wetting phases show an exponential decrease in resistivity, although the curves show significant variations between different cycles.

B. Test 2a

For Test 2a, the drive current was kept at 250µA, and the orientation of the Theta probe was restored as horizontal.

The location of both sensors was modified, moving them closer together. This was to try to obtain more consistent readings, as there was some concern that wetting of the sand was not occurring uniformly with time across the column. Figure 9 includes the resistivity-water content curves of three of the six cycles made for Test 2a. It can be seen that there is an improvement in the consistency and repeatability over the wetting phases compared with Test 1.

Resistivity continues to show an exponential trend, decreasing as water content increases over all the cycles. Responses during re-wetting decrease in resistivity as the water content increases up to 30%, then flatten up to 34%, while all draining cycles decrease exponentially from 34% to 12% water content. The re-wetting cycles still show some variability between successive cycles. The draining cycles seem to be missing readings at 33%, where there was an unexpected decrease in resistivity that was not recorded by the TF cell since it was outside of its working range.

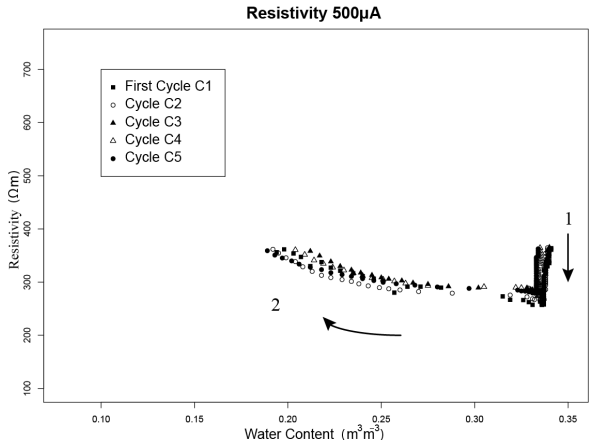

Figure 6. Water content - resistivity curves for all 500µA cycles.

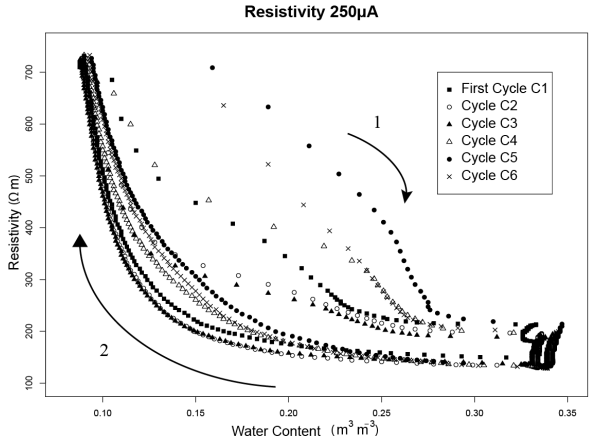

Figure 7. Water content - resistivity curves for all 250µA cycles.

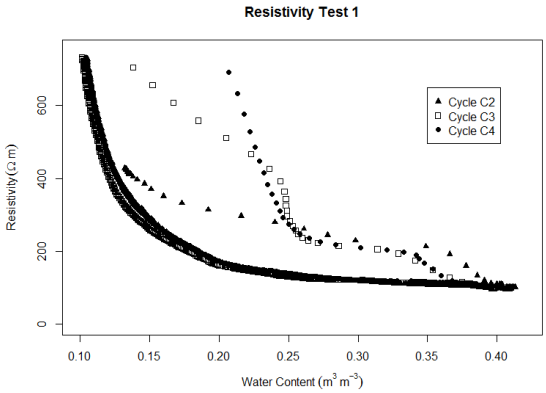

Figure 8. Water content - resistivity curves for Test 1 cycles.

C. *Test 2b*

Keeping the same configuration of Test 2a for the apparatus, Test 2b includes a change of drive current provided to the TF cell. As previously stated, the objectives of Test 2b were to use a drive current of 150µA to keep all readings within the range of the conductivity sensor output.

As can be seen in Figure 10, the range of the resistivity registered for all cycles is virtually double that of the previous experiments, preliminary and Test 1 (100Ωm-720Ωm) and almost triple that from Test 2a (50Ωm-480Ωm) ranging from 200Ωm to 1500Ωm. Re-wetting and re-drying phase's responses both follow the same trend with decreasing resistivity as water content is increasing.

However, re-drying phases again have lower resistivity readings compared to re-wetting readings. Measurements were taken at same 5-second intervals in both phases showing that the draining phase is much slower. The classic exponential trend is more explicit over the re-drying than re-wetting phases. There is an apparent hysteresis when responses of wetting and drying phases are compared in Figure 10; while there seems to be a good repeatability over consecutive cycles the responses follow different trends on each phase.

The TF cell gives different values of resistivity at the same water content being measured, e.g., in Figure 10 it is clearly seen that at 20% water content the value of resistivity is approximately 500Ωm and 900Ωm for wetting and draining phases respectively.

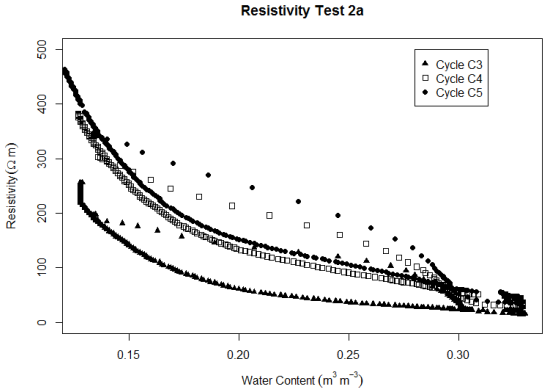

Figure 9. Water content - resistivity curves for Test 2a cycles.

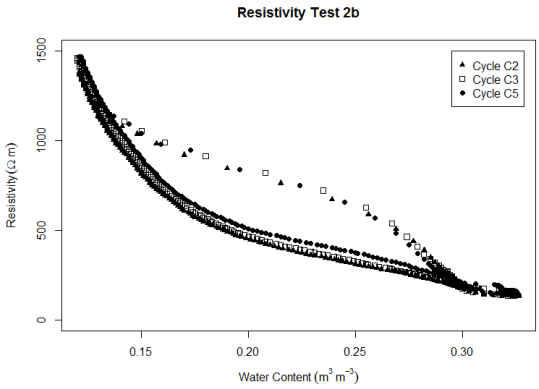

Figure 10. Water content - resistivity curves for Test 2b cycles.

A theory to explain this behaviour is shown in Figure 12a. Water is being added rapidly at the top of the column and allowed to drain at the bottom using only a small hose. Air trapped in the soil finds it difficult to escape, causing the water infiltration to be non-uniform. Figure 12b shows the sample between the electrodes of the TF cell when water is added at the top of the column, and Figure13b when water is added slowly from the bottom. The air that may stay trapped in the soil sample on rapid downward infiltration is the possible cause of the variation of the TF readings in the wetting phase, and this theory is supported by the results obtained on changing the direction of the water in the wetting phase of Test 3.

D. *Test 3*

For this test, the drive current was kept as 150µA, and the direction of filling was modified by adding water from the bottom, going up through the soil sample at an average flow rate of $7.68e^{-6}m^3/s$ until a water column of 0.15m height was formed at the top of the soil sample before draining started. The average drainage flow rate was a bit higher than filling with a value of $8.99e^{-6}m^3/s$.

Figure 11 shows water content-resistivity curves for three of the eight complete re-wetting and re-draining cycles. It can be seen that curves during wetting and drying phases both follow the same exponential trend of decrease in resistivity as soil water content increases.

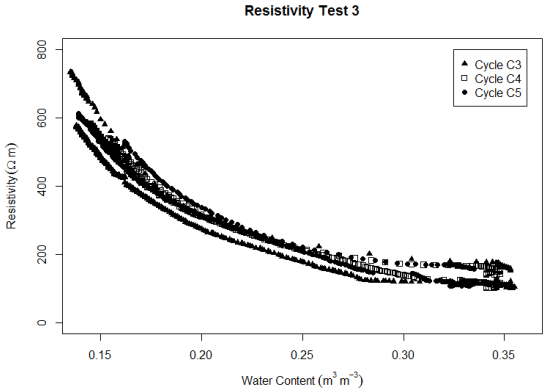

Figure 11. Water content - resistivity curves for Test 3 cycles.

 ISBN: 978-1-61208-581-4

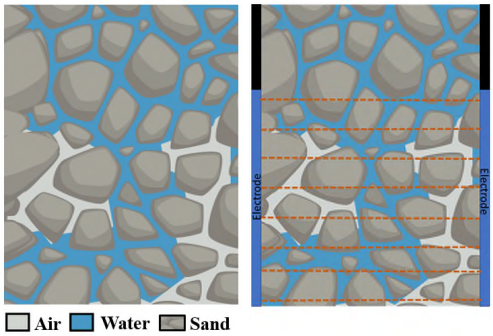

Figure 12. (a) Soil sample showing non-uniform downwards water infiltration, (b) non-uniform composition of soil/water between the TF electrodes.

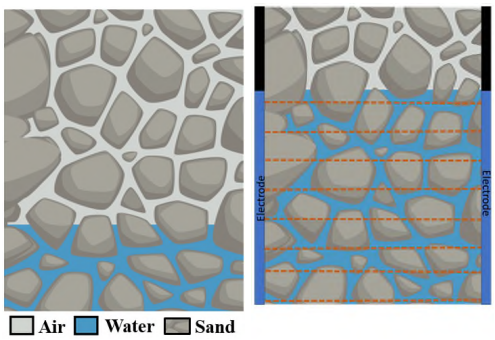

Figure 13. (a) Soil sample showing uniform upwards water infiltration, (b) uniform composition of soil/water between the TF electrodes.

However, the range of values over each phase are slightly different ranging from 200Ωm to 750Ωm for wetting, and 100Ωm to 600Ωm for drying. As explained previously, this may be because air is no longer trapped in the soil sample when the water is added from the bottom of the column, as is shown in Figure 13a. As the water surface moved upward, it pushed the air in the soil sample uniformly to the top of the open column.

IV. CONCLUSION

The Preliminary Test, along with Test 1 and 2a had the purpose of establishing the correct set-up of the experimental apparatus, including drive current and physical location of the sensors. The results from these have demonstrated the importance of setting the correct drive current for the TF cell. Test 2b and 3 compared the responses of the TF cell under two different water infiltration paths, downwards and upwards respectively, and this difference in the wetting method has created an interesting difference in the resistivity readings; the hypothesis of trapped air being the cause needs to be further investigated.

Resistivity measured using the output of the TF cell follows the trends in the available literature, including McCarter (1984) [16] and more recently Hen-Jones et al. (2017) [3], that show resistivity-water content trends for compacted clays. These can be seen in Figure 2 which summarises both works. The values of resistivity in Figure 2 are considerably lower than the values obtained in all experiments using TF cell. However, the soil samples used in this paper are sand instead of clay. Higher values were expected and correspond to soil resistivity generally having higher values in the sand than in clay soil samples.

Following the results presented, future work includes characterization of the response for different soil particle sizes and types (sand to clay), and relation to fundamental models including parameters of the soil such as density, porosity, saturation and compaction degrees.

ACKNOWLEDGMENT

Authors express their gratitude to the Mexican National Council for Science and Technology (CONACYT), the UK Engineering and Physical Sciences Research Council (EPSRC), and the Rail Safety and Standards Board (RSSB), who have all supported this work.

REFERENCES

[1] S. Glendinning, J. Hall, and L. Manning, “Asset-management strategies for infrastructure embankments,” In Proceedings of the Institution of Civil Engineers-Engineering Sustainability, vol. 162, no. 2, pp. 111-120, 2009.

[2] J. Perry, M. Pedley, and M. Reid, “Infrastructure embankments: condition appraisal and remedial treatment,” Construction Industry Research and Information Association. 2001.

[3] R. M. Hen-Jones, et al., “Seasonal effects on geophysical–geotechnical relationships and their implications for electrical resistivity tomography monitoring of slopes,” Acta Geotechnica, pp. 1-15, 2017.

[4] J. K. Atkinson, A. W. J. Cranny, W. V. Glasspool, and J. A. Mihell, “An investigation of the performance characteristics and operational lifetimes of multi-element thick film sensor arrays used in the determination of water quality parameters,” Sensors and Actuators B: Chemical, vol. 54, no. 3, pp. 215-231, 1999.

[5] J. K. Atkinson, et al., “Thick film screen printed environmental and chemical sensor array reference electrodes suitable for subterranean and subaqueous deployments,” Microelectronics International, vol. 30, no. 2, pp. 92-98. 2013.

[6] A. Gac, J. K. Atkinson, Z. Zhang, and R.P. Sion, “A comparison of thick-film chemical sensor characteristics in laboratory and on-line industrial process applications,” Measurement Science and Technology, vol. 13, no. 12, pp. 2062. 2002.

[7] C. M. Gardner, D. A. Robinson, K. Blyth, and J. D. Cooper, “Soil water content. Soil analysis: physical methods,” pp. 1-74.

[8] R. D. Grisso, M. M. Alley, D. L. Holshouser, and W. E. Thomason, “Precision farming tools. Soil electrical conductivity,” Available at https://pubs.ext.vt.edu/442/442-508/442-508_pdf.pdf (verified 2017.08.15), 2005.

[9] National Resources Conservation Service (NRCS), “Inherent factors affecting soil EC,” Soil Electrical Conductivity, Available at

http://www.nrcs.usda.gov/Internet/FSE_DOCUMENTS/nrcs142p2_053280.pdf (verified 2017.08.15).

[10] J. D. Rhoades, N. A. Manteghi, P. J. Shouse, and W. J. Alves, "Soil electrical conductivity and soil salinity: new formulations and calibrations," Soil Science Society of America Journal, vol. 53, no. 2, pp. 433-439, 1989.

[11] V. Lapenna, et al., "High-resolution geoelectrical tomographies in the study of Giarrossa landslide (southern Italy)," Bulletin of Engineering Geology and the Environment, vol. 62, no. 3, pp. 259-268, 2003.

[12] Y. Mao, E. Romero, and A. Gens, "Exploring ice content on partially saturated frozen soils using dielectric permittivity and bulk electrical conductivity measurements," The third European Conference on Unsaturated Soil – E-UNSAT 2016 vol. 9, pp. 1-6, 2016.

[13] K. Suzuki and S. Higashi, "Groundwater flow after heavy rain in landslide-slope area from 2-D inversion of resistivity monitoring data," Geophysics, vol. 66, no. 3, pp. 733-743, 2001.

[14] D. L. Corwin and S. M. Lesch, "Apparent soil electrical conductivity measurements in agriculture," Computers and Electronics in Agriculture, vol. 46, no. 1, pp. 11-43, 2005.

[15] M. Sophocleous and J. K. Atkinson, "A novel thick-film electrical conductivity sensor suitable for liquid and soil conductivity measurements," Sensors and Actuators B: Chemical, vol. 213, pp. 417-422, 2015.

[16] W. J. McCarter, "The electrical resistivity characteristics of compacted clays," Géotechnique, vol. 34, no. 2, pp. 263-267, 1984.

 ISBN: 978-1-61208-581-4